# Halofuginone Inhibits Angiogenesis and Growth in Implanted Metastatic Rat Brain Tumor Model—an MRI Study[1]

*Rinat Abramovitch*, Anna Itzik[†], Hila Harel*[,‡], Arnon Nagler[‡,§], Israel Vlodavsky[¶] and Tali Siegal[†,‡]*

*The Goldyne Savad Institute of Gene Therapy, and MRI/MRS Laboratory, HBRC, Hadassah Hebrew University Medical Center, Jerusalem, Israel; [†]The Leslie and Michael Gaffin Center for Neuro-Oncology, Hadassah Hebrew University Medical Center, Jerusalem, Israel; [‡]Sharett Institute of Oncology, Hadassah Hebrew University Medical Center, Jerusalem, Israel; [§]Departments of Hematology and Bone Marrow Transplantation, Chaim Sheba Medical Center, Tel-Hashomer, Israel; [¶]Cancer and Vascular Biology Research Center, Rappaport Faculty of Medicine, Technion, Haifa, Israel

## Abstract

**Tumor growth and metastasis depend on angiogenesis; therefore, efforts are made to develop specific angiogenic inhibitors. Halofuginone (HF) is a potent inhibitor of collagen type α1(I). In solid tumor models, HF has a potent antitumor and antiangiogenic effect *in vivo*, but its effect on brain tumors has not yet been evaluated. By employing magnetic resonance imaging (MRI), we monitored the effect of HF on tumor progression and vascularization by utilizing an implanted malignant fibrous histiocytoma metastatic rat brain tumor model. Here we demonstrate that treatment with HF effectively and dose-dependently reduced tumor growth and angiogenesis. On day 13, HF-treated tumors were fivefold smaller than control ($P < .001$). Treatment with HF significantly prolonged survival of treated animals (142%; $P = .001$). In HF-treated rats, tumor vascularization was inhibited by 30% on day 13 and by 37% on day 19 ($P < .05$). Additionally, HF treatment inhibited vessel maturation ($P = .03$). Finally, in HF-treated rats, we noticed the appearance of a few clusters of satellite tumors, which were distinct from the primary tumor and usually contained vessel cores. This phenomenon was relatively moderate when compared to previous reports of other antiangiogenic agents used to treat brain tumors. We therefore conclude that HF is effective for treatment of metastatic brain tumors.**

*Neoplasia* (2004) **6**, 480–489

**Keywords:** MRI, brain tumor, angiogenesis, halofuginone, vessel cooption.

## Introduction

Patients with malignant primary and metastatic brain tumors have poor prognosis, despite developments in diagnostic and therapeutic modalities. Conventional therapy is seldom curative and, therefore, a search for new therapeutic avenues is ongoing. The inhibition of angiogenesis—the sprouting of new capillaries from pre-existing vasculature—seems to offer a promising approach to tumor growth arrest [1,2]. Its relevance is derived from the observation that most tumors and metastases originate as small avascular masses that later induce the development of new blood vessels once they grow beyond a few millimeters in size [3]. Furthermore, high-grade brain tumors are characterized by endothelial proliferation and a high degree of vascularity. In these tumors, the amount of neovasculature is closely correlated with the degree of malignancy and the prognosis of the patient [4–6].

Collagen type I, a major component of the extracellular matrix (ECM), plays an important role in the proliferation and invasion of endothelial cells (ECs) [7]. A marked increase in the transcription of type I collagen was demonstrated in ECs undergoing angiogenesis [8] and blockage of collagen secretion inhibited EC migration [9]. Experimentally, capillary ECs reorganize into a network of branching and anastomosing capillary-like tubes when sandwiched between two layers of type I collagen gel [10]. When the collagen type I fibrils make contact with the apical side of the endothelium, they act as a stimulus to provide a template for vascular tube formation [11]. The receptors for the native collagen, the $\alpha_1\beta_1$ and $\alpha_2\beta_1$ integrins, are highly expressed by ECs during angiogenesis. Antibodies that block these receptors selectively inhibit vascular endothelial growth factor (VEGF)-driven angiogenesis without affecting pre-existing vasculature [12]. Halofuginone (HF), a low-molecular-weight ($M_W$ = 495) quinazolinone alkaloid, is a potent inhibitor of collagen type α1(I) synthesis at the transcriptional level [13,14]. In culture, HF has been found to attenuate collagen α1(I) gene expression and collagen production. It inhibits vascular tube formation and, accordingly,

Abbreviations: BOLD, blood oxygenation level–dependent; CNS, central nervous system; EC, endothelial cell; HF, halofuginone; MRI, magnetic resonance imaging; SMA, smooth muscle actin; VEGF, vascular endothelial growth factor; VD, vasodilation; VF, vascular function

Address all correspondence to: Rinat Abramovitch, PhD, The Goldyne Savad Institute of Gene Therapy, Hadassah Hebrew University Medical Center, PO Box 12000, Jerusalem 91120, Israel. E-mail: rinat@hadassah.org.il

[1]The research described in this article was supported, in part, by Collgard Biopharmaceuticals Ltd., the Belfer Foundation (R.A.), Philip Morris Incorporated fellowship program (R.A.), the Horowitz Foundation for complexity science (R.A.), and Yael Research Fund c/o Biosense Ltd. (R.A.).

Received 20 December 2003; Revised 26 February 2004; Accepted 3 March 2004.



DOI 10.1593/neo.03520

was found to be an inhibitor of both angiogenesis and tumor growth in *in vitro* models. *In vivo*, it has potent antitumor and antimetastatic effects in systemic solid tumor models [15–17].

In the past, several antiangiogenic agents have shown an inhibitory effect in numerous experimental models [16,18–20]. However, when evaluating antiangiogenic strategies in animal models, one must consider that the morphology and function of the tumor vasculature are largely dependent upon the host environment. As some primary central nervous system (CNS) tumors often show a highly infiltrative growth pattern, it raises the question of whether the vessels in such tumors are formed by angiogenesis or are pre-existent ones. Indeed, the use of pre-existent vessels in early metastatic outgrowths in the brain, a process referred to as vessel cooption, has been reported [21,22]. As these tumors progress, they switch to an angiogenic phenotype and new vessels penetrate from the surrounding vasculature. In this regard, it is important to realize that most antiangiogenic studies have been carried out in animal models where tumors were grown subcutaneously. Especially for CNS tumor biology, subcutaneous models have limited clinical relevance since the subcutaneous space is essentially avascular. Thus, the subcutaneous tumors are artificially selected to grow in an angiogenic-dependent fashion, whereas the microenvironmental conditions that exist in the brain are of a highly vascularized nature.

There are few models for studying brain metastasis. The model of internal carotid artery injection of tumor cells is one of the suitable biologic models for metastatic dissemination [22]. However, with such a model, the locations and sizes of the lesions are heterogeneous and unpredictable. Thus, for the study of antitumor effect of a new drug, the use of a model with a precisely known location, size, and growth kinetics is of great advantage. We chose to work with a well-characterized model that uses cells of malignant fibrous histiocytoma, which are injected into the right cerebral hemisphere [23,24]. The tumors that consequently develop behave like a metastatic brain lesion, and its exact location and size at each time point are well characterized.

Noninvasive magnetic resonance imaging (MRI) has demonstrated the capability to perform repeated measurements of tumors implanted intracranially and to measure changes caused by therapies [25–28]. MRI methods facilitate detectability of changes in tumor vascularization, in addition to their traditional role of measuring tumor volume. There are few approaches to study antivascular effects by MRI: permeability to contrast agents [27–31], diffusion-weighted MRI [32], $T_{1\rho}$-weighted method [33], and blood oxygenation level–dependent (BOLD) contrast [16,25,34,35]. BOLD-MRI is based on changes in proton signals from tissue that is adjacent to blood vessels containing paramagnetic deoxyhemoglobin [36]. Unlike oxyhemoglobin, which is diamagnetic and has minimal effect, deoxyhemoglobin is paramagnetic and acts as a $T_2^*$ relaxing agent. Therefore, the changes in tissue levels of deoxyhemoglobin cause local magnetic field susceptibility gradients, which can be detected as changes in MRI signal intensities. These changes correlate with fluctuations in oxygen saturation, blood flow, and blood volume [37].

The goal of this study was to evaluate the ability of HF to inhibit tumor growth in a metastatic rat brain tumor model. By using MRI, we noninvasively monitored the effect of HF on tumor progression and vascularization. We have selected to use BOLD imaging, a functional MRI technique, which is susceptible to tumor perfusion, oxygenation, and vessel reactivity (response to $CO_2$). We have previously used this method to study tumor angiogenesis and vessel maturation [16,35,38]; however, so far, it has not been applied for the evaluation of HF effects on intraparenchymal brain tumors. In this study, we demonstrate that treatment with HF reduced tumor growth and angiogenesis of an intracranially implanted malignant sarcoma in rats and thus prolonged the survival of treated rats.

## Materials and Methods

### *Materials*

HF bromohydrate was obtained from Collgard Biopharmaceuticals Ltd. (Petach-Tikva, Israel).

### *Tumor Cell Line*

The tumor used for the *in vivo* experiments is an unselected rat tumor line of a methylcholantrene-induced malignant fibrous histiocytoma as reported previously [23]. The tumors used for *in vivo* experiments were maintained in syngeneic Fischer rats by serial subcutaneous transplantations. Tumor cell suspension was prepared as previously described, assayed for viability by the Trypan blue exclusion test, and resuspended at the appropriate inoculum concentration in RPMI medium. Tumor cells were maintained subcutaneously because in tissue culture, these cells change their phenotype rapidly. Limited numbers of passages were used. The same cell suspension was used each time to inject an equal number of controls and the experiment group of HF treatment.

### *Stereotactic Brain Inoculation*

Adult female Fischer rats (weighing 180–200 g) were anesthesized by intraperitoneal injection of 30 mg/kg pentobarbital; the tumor cell suspension was injected into the right cerebral hemisphere, using a small animal stereotactic apparatus. With bregma as zero reference point, the stereotactic coordinates were $P = 3.5$, $L = 2$, and $H = -4$ mm, as previously described [24]. Those coordinates targeted the tumor cells to the subcortical white matter. The head was held in a horizontal position and $10^5$ tumor cells suspended into a 2-$\mu$l volume were injected. Tumor cells were injected slowly for 10 minutes to avoid an acute elevation of intracranial pressure or upward solution leakage through the track of the injecting needle.

### *Animal Protocols*

Treatment with HF was initiated on day 6 after tumor implantation, a time when a macroscopic tumor mass had

already developed [24]. Oral treatment (by oral gavage) was given daily until animals were sacrificed (for histology analysis) or left to die (for survival). Animals were observed for signs of toxicity and weight loss. Rats were housed in cages at 20°C with a 12-hour light/dark schedule, and free access to food and water. Animal experiments were approved by the Animal Care Committee of the Hebrew University Faculty of Medicine.

*Dose evaluation* Four groups were evaluated: 1) vehicle; 2) HF, 0.1 mg/kg per day; 3) HF, 0.2 mg/kg per day; and 4) HF 0.4 mg/kg per day ($n$ = 10 per group). Rats were sacrificed on day 14. Visible tumor was excised and its three dimensions were measured for calculation of tumor volume. HF plasma levels were determined on days 7 and 14. Animals were observed for signs of toxicity and weight loss. Tissue samples of lung, liver, heart, kidney, brain, and spleen were obtained from each experimental group and evaluated histologically for signs of toxicity.

*Survival* Survival was evaluated after randomization to treatment with either vehicle or HF (0.2 and 0.4 mg/kg per day). Treatment was started on day 6 and continued until death ($n$ = 12 for each treatment group).

*MRI* For MRI experiments, only two groups were used: 1) vehicle and 2) HF, 0.4 mg/kg per day. MRI scans were performed on days 13, 17, and 19 after tumor implantation.

*Histology*

Anesthesized animals were perfused transcardially with 20 ml of formalin. Brains were removed and immersed in the same fixative overnight at 4°C. Coronal sections (5 μm) were cut and stained with hematoxylin and eosin.

*Immunohistochemistry*

Paraffin-embedded tumor sections were stained for α-smooth muscle actin (α-SMA) (Sigma Chemical Co., St. Louis, MO), in a 1:2500 dilution, to detect vascular smooth muscle cells and pericytes. Blood vessels were detected by either *Bandeiraea simplicifolia* BS-1 Isolectin (LEC; 1:10 dilution) or antibody to factor VIII (von Willebrand factor, vWF) (DAKO, Glostrup, Denmark). The vWF antibody was used in a 1:200 dilution after treating the section with proteinase K for 10 minutes at 37°C.

*MRI Analysis of Tumor Volume, Blood Vessel Functionality, and Vessel Maturation*

MRI experiments were performed on a horizontal 4.7T Biospec spectrometer (Bruker Medical, Ettlingen, Germany) using an actively radiofrequancy-decoupled surface coil (2 cm in diameter) and a birdcage transmission coil [35]. Rats were anesthesized (pentobarbital, intraperitoneally) and placed in a prone position with the brain located at the center of the surface coil. Ten rats per group were imaged on days 13, 17, and 19 after tumor cell inoculation. Intracranial tumor volume was determined from multislice coronal and axial fast spin-echo images (repetition time = 2000 milliseconds, echo time = 45 milliseconds, slice thickness = 0.85 mm, and field of view = 3.4 cm, using a 256 × 128 matrix). In brief, the tumor boundary visualized in each slice was outlined by using image processing software (NIH Image, Bethesda, MD). The number of tumor pixels was converted to an area by multiplication by the factor [(field of view)$^2$ / (matrix)$^2$]. The total tumor volume was calculated as the summed area on all slices, multiplied by the slice thickness [39]. Tumor borders were also confirmed with $T_1$-weighted inversion recovery sequence (repetition time = 2000 milliseconds, echo time = 45 milliseconds, inversion delay = 250 milliseconds).

Tumor vascular function (VF) and maturation (VD) were determined from gradient-echo (GE) images acquired during the inhalation of air, air−$CO_2$ (95% air and 5% $CO_2$), and oxygen−$CO_2$ (95% oxygen and 5% $CO_2$; carbogen), as described [35]. Four images were acquired at each gas mixture (51 sec/image; slice thickness = 0.85 mm; TR = 100 milliseconds; TE = 10 milliseconds; field of view = 3 cm; 256 × 128 pixels; in-plane resolution = 110 μm; four averages). Other imaging experimental details were as reported previously [35,40].

*Data Analysis*

MRI data were analyzed on a PC computer using IDL software (Research Systems Inc., Boulder, CO). VF was derived from images acquired during inhalation of carbogen and air−$CO_2$ as described previously [35,40], using the following equation:

$$\mathrm{VF} = b\Delta Y = \ln(I_{\mathrm{oxygen}}/I_{\mathrm{air}})/\mathrm{TE} \times C_{\mathrm{MRI}}$$

where $I_{\mathrm{oxygen}}$ and $I_{\mathrm{air}}$ are the mean signal intensity during inhalation of oxygen and air, respectively; TE is the echo time; $Y$ is the fraction of oxyhemoglobin; $b$ is the volume fraction of blood; and $C_{\mathrm{MRI}}$ is a factor representing magnetic field strength. This parameter measures the capacity of erythrocyte-mediated oxygen delivery from the lungs to each pixel in the image [35,40].

*Vascular maturation* is demonstrated by vasodilation (VD) in response to change of $CO_2$ levels (from images acquired during inhalation of air and air−$CO_2$), as described [35,40]:

$$\mathrm{VD} = \ln(I_{\mathrm{air-CO_2}}/I_{\mathrm{air}})/\mathrm{TE} \times C_{\mathrm{MRI}}$$

Positive VD corresponds to increased signal intensity by hypercapnia, due to elevated blood oxygenation and/or increased blood flow [40]. Data are presented in color maps overlaid on the original baseline image for absolute values of VD and VF >0.005 [35]. Mean VF and VD values were calculated from the entire tumor and were divided by the mean values from a corresponding region with the same size taken at the homologous contralateral side.

*Statistics*

Results are expressed as mean ± SD. Differences between groups were identified by the unpaired Student's $t$ test. A $P$ value of less than .05 was considered statistically significant. Tumor volume, VF, and VD data were analyzed after

normalization with logarithmic transformation. Considering the repeated measurements on the same animals, we used an appropriate repeated measurement model. Least squares means for each day (13, 17, and 19) that resulted from the statistical model were compared in order to find the difference between the experimental groups. The Bonferroni method was used to correct for repeated measurements. The statistical significance of differences in survival time was analyzed by means of the Wilcoxon ranking test.

## Results

*Effect of HF on Tumor Growth*

The day of inoculation of tumor cells was considered day 0. Oral treatment with HF was initiated on day 6 after tumor cell implantation, a time when a macroscopic tumor mass had already developed [24], and repeated daily. On day 14, tumors were excised ($n = 10$ per group) and their volume was calculated by measurements of the tumor's three dimensions on serial sectioning. Mean brain tumor volume of vehicle-treated animals (controls) was 49.4 ± 8.4 $mm^3$. Treatment with HF induced dose-related inhibition of tumor growth: 49% inhibition of tumor growth in dose of 0.1 mg/kg per day ($P = .06$), 88% inhibition in dose of 0.2 mg/kg per day ($P = .0005$), and 94% inhibition at dose of 0.4 mg/kg per day ($P = .0001$). Mean HF plasma levels on day 14 were: 1.32 ± 0.4 ng/ml for dose of 0.1 mg/kg per day, 2.27 ± 0.3 ng/ml for dose of 0.2 mg/kg, and 4.53 ± 1.02 ng/ml for dose of 0.4 mg/kg. All animals lost weight during the observation period. Weight loss ranged between 9% and 13% of initial body weight and did not differ significantly between untreated tumor-bearing controls and HF-treated animals. No drug-related toxicity was observed on histologic evaluation of the internal organs.

In order to study the kinetics of the effect of HF on tumor growth, we used MRI, which is a noninvasive technique. Oral treatment with HF (0.4 mg/kg per day) was initiated on day 6 after tumor cell implantation and repeated daily. MRI studies were performed on days 13, 17, and 19 after cell implantation (10 rats per group). Indeed, MRI confirmed the delay in tumor growth in HF-treated rats in comparison to control rats (Figure 1; Bonferroni $P < .001$ for all time points). In vehicle-treated rats, exponential growth of the tumors was observed and, on day 19, they covered most of the ipsilateral hemisphere (Figure 1*C*). A significant inhibition of tumor growth was detected during the observation period in HF-treated rats. On day 13, HF-treated tumors were fivefold smaller than control (Figure 1, *B* and *A*, respectively), and remained threefold smaller on days 17 and 19 (Figure 1, *D* and *C*, respectively). It should be noted that in some cases, in control-treated rats, the tumor erupted from the skull—a phenomenon that never occurred in HF-treated rats. Tumor volume was calculated only from the intracranial mass.

*Effect of HF on Rat Survival*

As a consequence of growth inhibition, HF treatment significantly prolonged survival of brain tumor-bearing rats (Figure 2). The median survival of vehicle-treated animals was 19 days (range: 15–22 days), while median survival of the 0.2 mg/kg per day HF group was 21 days (range: 17–26 days) ($P = .002$) and of the 0.4 mg/kg per day treatment group was 27 days (range: 21–31) ($P = .0001$). The increase in lifespan of the 0.4 mg/kg per day group is 142%. The difference between the two treatment groups (0.2 and 0.4 mg/kg) is also significant ($P = .001$).

*Effect of HF on Tumor Angiogenesis and Vessel Maturation*

The brain is one of the most vascularized organs with a well-oxygenated blood supply. Malignant brain tumors are frequently characterized by well-perfused, high-density vascular bed [41]. We evaluated the effect of HF on tumor vascularization and, indeed, the delay in tumor growth was accompanied by reduced vascularization in HF-treated tumors, as determined by VF maps (Figure 3). In HF-treated rats, tumor vascularization was inhibited by 50% on day 13 and by 37% on day 19 (Figure 3; VF). Using the Bonferroni method (correction for repeated measurements) revealed statistically significant influence of HF on tumor vascularization ($P < .05$).

The higher vascularization of control vs. HF-treated tumors was confirmed by immunostaining of histologic sections with both lectin and anti–factor VIII antibody (Figure 4, *A–D*). Microvessel counts revealed that on day 13, the mean count per × 40 microscopic field was 16.0 ± 3.5 for controls and 7.5 ± 1.8 vessels, for the HF group ($P = .00001$). On day 19, there were less vessels in each field, 9.5±2 vessels in controls vs. 6.0 ± 2.8 vessels in HF-treated tumors ($P = .03$, two tumors per group, 10 fields per tumor). In addition, on day 19, control tumors contained larger vessels (Figure 4*C*, *insert*) as compared with the HF-treated ones.

Using MRI, we were also able to study the effects of HF on vessel maturation. In control tumors, vessel maturation progressed from the tumor margins inwards and the percent of mature vessels increased from days 14 to 19 by approximately 50%. HF treatment significantly inhibited vessel maturation (Bonferroni $P = .03$) (Figure 3; VD). These results were confirmed by staining tissue sections with α-SMA antibody (Figure 4, *E* and *F*). There were few blood vessels, which stained positively with α-SMA antibody within control tumors (Figure 4*E*, *red arrows*). At the same time, in the HF-treated tumors, we could find no mature vessels within the tumor mass. However, numerous α-SMA positive mature vessels were observed in the vicinity of the HF-treated tumor mass, which were covered with few layers of tumor cells (cooption) (Figure 4*F*, *red arrows*).

*Effect of HF on Tumor Morphology*

The tumors used for our studies usually grew as relatively well-circumscribed intraparenchymal masses in Fischer rats [24] (Figures 1 and 4). In HF-treated rats, we observed a moderate 2.4-fold increase in the number of satellite tumors that were clustered around—but distinct from—the primary lesion (Figure 4, *B* and *F*, *black arrows*). These satellites were clustered around the main mass and usually contained discernible vessel cores (Figure 4*B*). On some sections, it could be

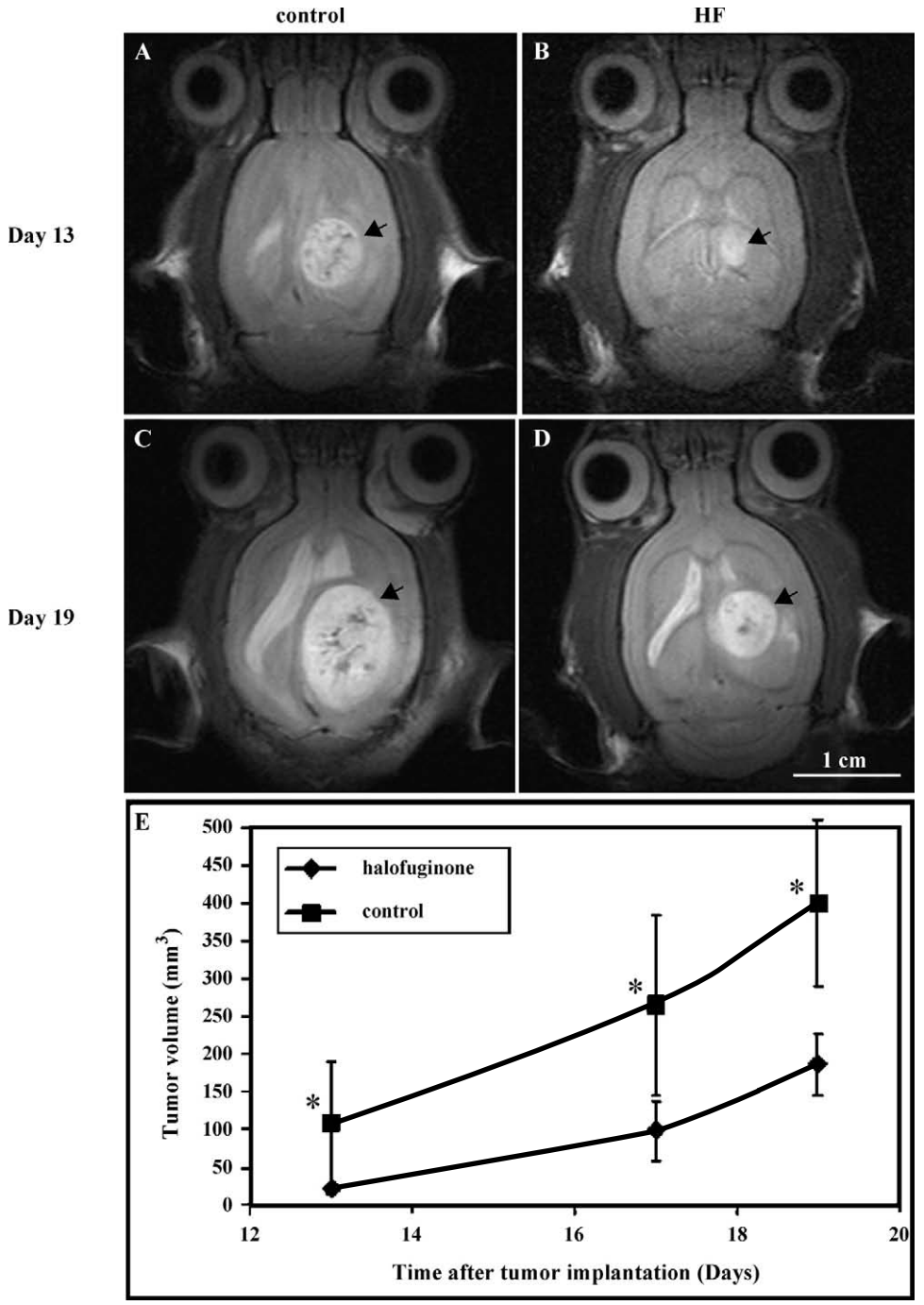


**Figure 1.** *HF inhibits tumor growth in a metastatic rat brain tumor model. Fischer rats were inoculated in the right cerebral hemisphere with $10^5$ malignant fibrous histiocytoma. Oral treatment with HF (0.4 mg/kg per day) or control vehicle was initiated on day 6 after tumor implantation, and treatment was repeated daily. Tumor growth kinetics was followed from consecutive fast spin-echo images (repetition time = 2000 milliseconds, echo time = 45 milliseconds, slice thickness = 0.85 mm, and field of view = 3.4 cm) of the tumor. Rats were scanned on days 13, 17, and 19 after tumor implantation. Representative axial $T_2$-weighted SE images of a control-treated rat (A and C) versus HF (0.4 mg/kg per day)–treated rat (B and D). Images were acquired on days 13 (A and B) and 19 (C and D) after cell inoculation (arrowhead = tumor; bar = 1 cm). (E) Mean tumor volume ($mm^3$) of HF-treated (♦) versus control (■), determined from SE images as a function of time after cell inoculation (n = 10 rats per group; *P < .001 for all time points).*

demonstrated that the satellites represented cross-sectioning of vessels that were surrounded over a long distance by a perivascular coat of tumor cells (Figure 4*F*, *arrow*).

## Discussion

Although conventional chemotherapeutic agents have a direct cytotoxic effect on tumor cells, they induce a high incidence of drug resistance as well as serious systemic adverse effects. In contrast, recent antiangiogenic substances, such as small molecule inhibitors, are less likely to develop drug resistance and serious side effects because they target only activated ECs on a molecular basis, instead of unselected cell population. Although the effect is temporary and cytostatic, these new agents inhibit angiogenesis

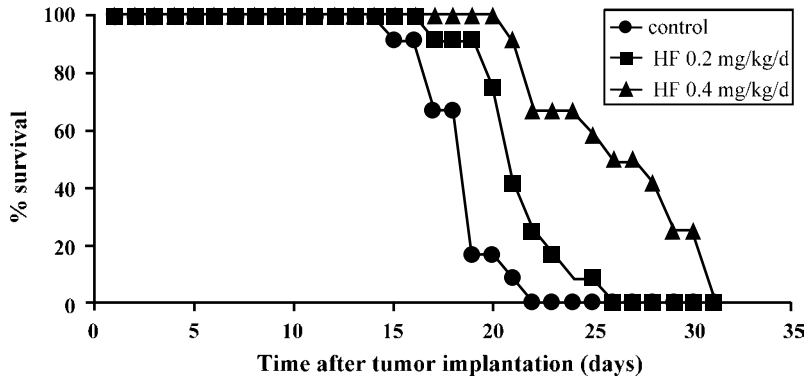


**Figure 2.** *Effect of HF on rat survival. Fischer rats were inoculated in the right cerebral hemisphere with $10^5$ malignant fibrous histiocytoma. Oral treatment with HF [0.2 mg/kg per day (■); 0.4 mg/kg per day (▲)] or control vehicle (●) was initiated on day 6 after tumor implantation, and treatment was repeated daily until animal death. Survival of the rats was monitored daily (n = 12 rats per group).*

and lead to small avascular tumors, which are maintained in a dormant state.

Brain tumors are highly angiogenic and dependent on neovascularization for their continued growth and invasion. Antiangiogenesis is thus a potentially important therapeutic strategy for these malignancies. In this study, we demonstrate that HF, an inhibitor of angiogenesis, is effective as a single therapeutic modality in an animal model with a metastatic brain tumor. We show that growth inhibition is dose-dependent and that tumor volumes in HF-treated rats were reduced by 88% to 94 % on day 14 after cell implantation in comparison to controls. This inhibitory effect could be demonstrated even when treatment was delayed and given at a time when a macroscopic tumor mass had already developed (day 6 after cell implantation) [24]. Concurrently, HF significantly prolonged rat survival. Our MRI analysis indicates that the inhibitory effect of HF on tumor growth was associated with a significant reduction of tumor angiogenesis and vessel maturation.

Ideally, treating an established human tumor with antiangiogenic therapy requires not only the inhibition of further angiogenesis, but also loss of existing tumor vessels to reduce the existing tumor mass. To recognize such an effect, features that distinguish a preformed tumor vasculature from host vessels are sought, and one such feature is the state of vessel maturation. It was shown previously that human brain tumors contain a significant fraction of immature vessels. In tumor specimens of glioblastoma multiforme, less than one quarter of tumor vessels, larger than capillaries, was associated with $\alpha$-SMA–positive cells [42]. The presence of a large fraction of immature vessels in these tumors was in sharp contrast to the normal brain, where the majority of vessels were covered by $\alpha$-SMA–positive cells [42]. From both MRI and histology results, it seems that HF reduces both the process of vessel maturation and its well-demonstrated antiangiogenic effect.

With the expeditious development of new antiangiogenic therapies, there is a growing need for noninvasive methods that will monitor the response of tumor vasculature to these biologic manipulations. Optimal treatment monitoring should rely on biologic endpoints, which indicate that angiogenesis is actually inhibited. The current study demonstrates that MRI could serve this purpose. We clearly show that MRI is a potential tool for *in vivo* monitoring not only of tumor volume, but also of tumor vascularization and the status of its vascular maturation. The use of BOLD contrast MRI for monitoring the effect of treatment with antiangiogenic drugs in animal tumor models was previously described [16,25,31,43]. Nevertheless, we demonstrate here that, even in the brain, a well-oxygenated organ, MRI provides a powerful noninvasive tool for monitoring treatment effects while exploiting changes in gas breathed.

Previous studies showed that the effects of HF on the growth and vascularization of subcutaneous C6 glioma were more dramatic than our current experience [16]. Indeed, the subcutaneous model is very useful to study basic principles of angiogenesis and antiangiogenesis, but it is unclear whether extrapolation of these results to the intracerebral localization is valid. Subcutaneous tumors characteristically grow in an encapsulated fashion while brain tumors tend to grow in a more infiltrative manner [44]. Thus, it is important to study the therapeutic effects in a more suitable environment that mimic the actual milieu for tumor growth. Our study indicates that HF is effective even when the tumor involves the brain parenchyma and it produces inhibitory effects on tumor growth similar to the previous findings in subcutaneous models.

Vessel cooption is thought to precede angiogenesis in the progression of astrocytomas and low-grade brain tumors [45]. In this work, tumor cells are mesenchymal in origin and their behavior is different from that of low-grade brain tumor. In this model, tumor progression is very rapid (the rats died 19 days postinjection) and is highly angiogenic. Only after HF treatment did we observe the appearance of vessel cooption, similar to what is known for untreated low-grade brain tumors. It seems that angiogenesis inhibition promotes tumor growth along pre-existing vessels, independently of neovascularization.

The hypothesis of a vascular dependency of tumors is very attractive, but it raises some unsolved issues related to

antiangiogenic treatment. For example, malignant glial tumors frequently show an infiltrative growth pattern [1]. The infiltrative trails include dissemination of tumor cells along existing tissue spaces and migration along blood vessels (vessel cooption). These tumor cells are likely to receive an adequate blood supply by the normal brain vasculature, thereby reducing the necessity to induce new vascular supply [1]. From these observations, it can be predicted that although the growth of the tumor bulk might be angiogenic-dependent, antiangiogenic therapy alone would be unlikely to succeed in killing all tumor cells.

Former experiments showed that gliomas could coopt pre-existent cerebral vessels to provide their blood supply, before they induce neovascularization [21]. In our work, we

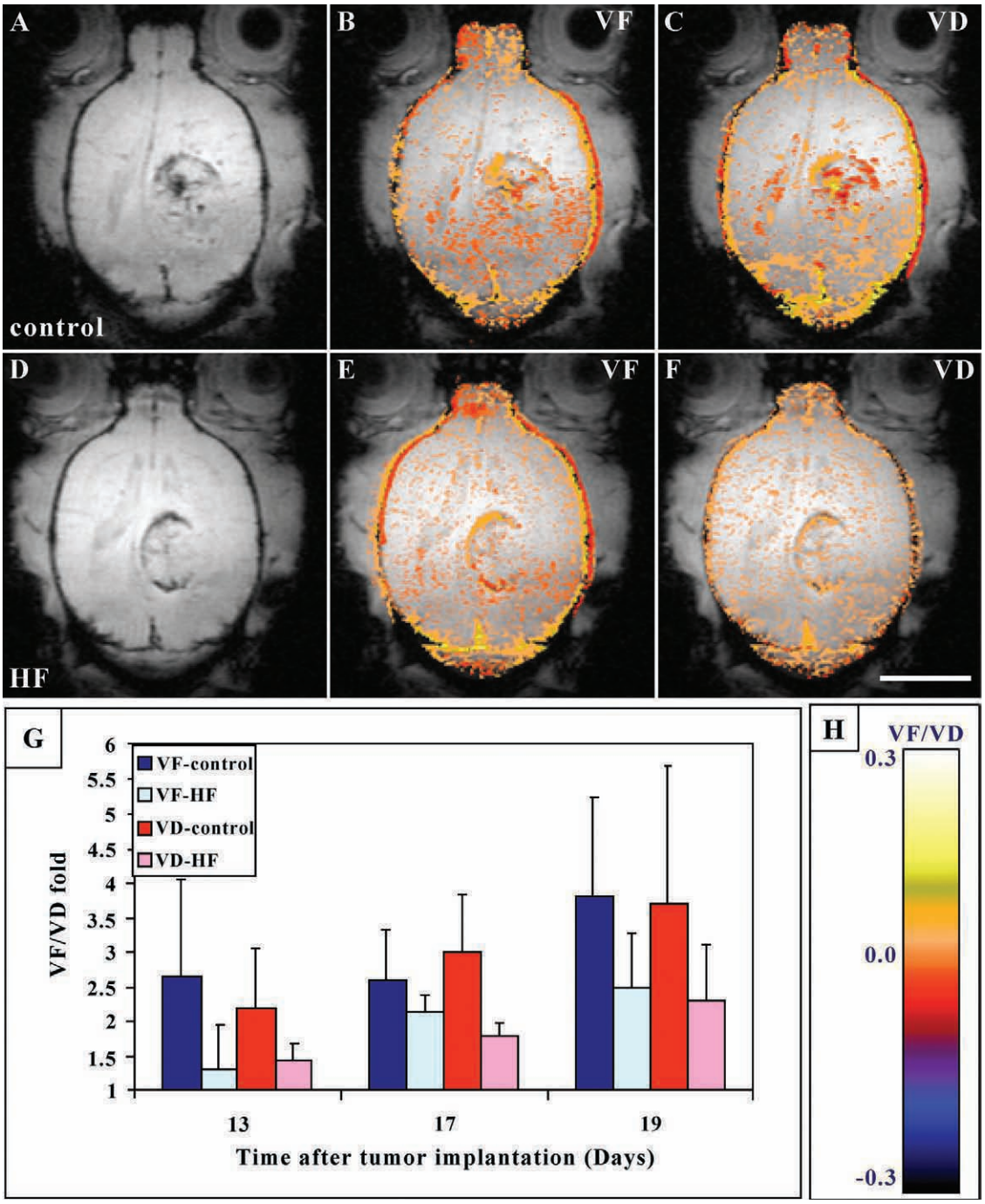


**Figure 3.** *Effect of HF on vascular function (VF) and maturation (VD) in metastatic brain tumors. Representative axial gradient echo (GE) images of control (A) and HF-treated (D) rats acquired on day 17 after tumor implantation. Functionality and maturation of the vasculature were derived from GE images acquired during inhalation of air, air–$CO_2$, and carbogen. Color-coded VF and VD maps were derived and overlaid [|VF| > .005; |VD| > .005; see color scale in (H)] on original images. Note the higher vessel density at the tumor periphery and the reduced vascular function (VF) and maturation (VD) in HF-treated tumors (E and F) versus controls (B and C) (bar = 1 cm). (G) Mean tumor VF and VD. The mean ± SD values of VF and VD were calculated from the region of interest containing the whole tumor and normalized as fold over values in normal brain, applying six rats per group and two to three slices per tumor. Bonferroni method (correction for repeated measurements) revealed statistically significant influences of HF on tumor vascularization (VF) and maturation (VD), $P < 0.05$.*

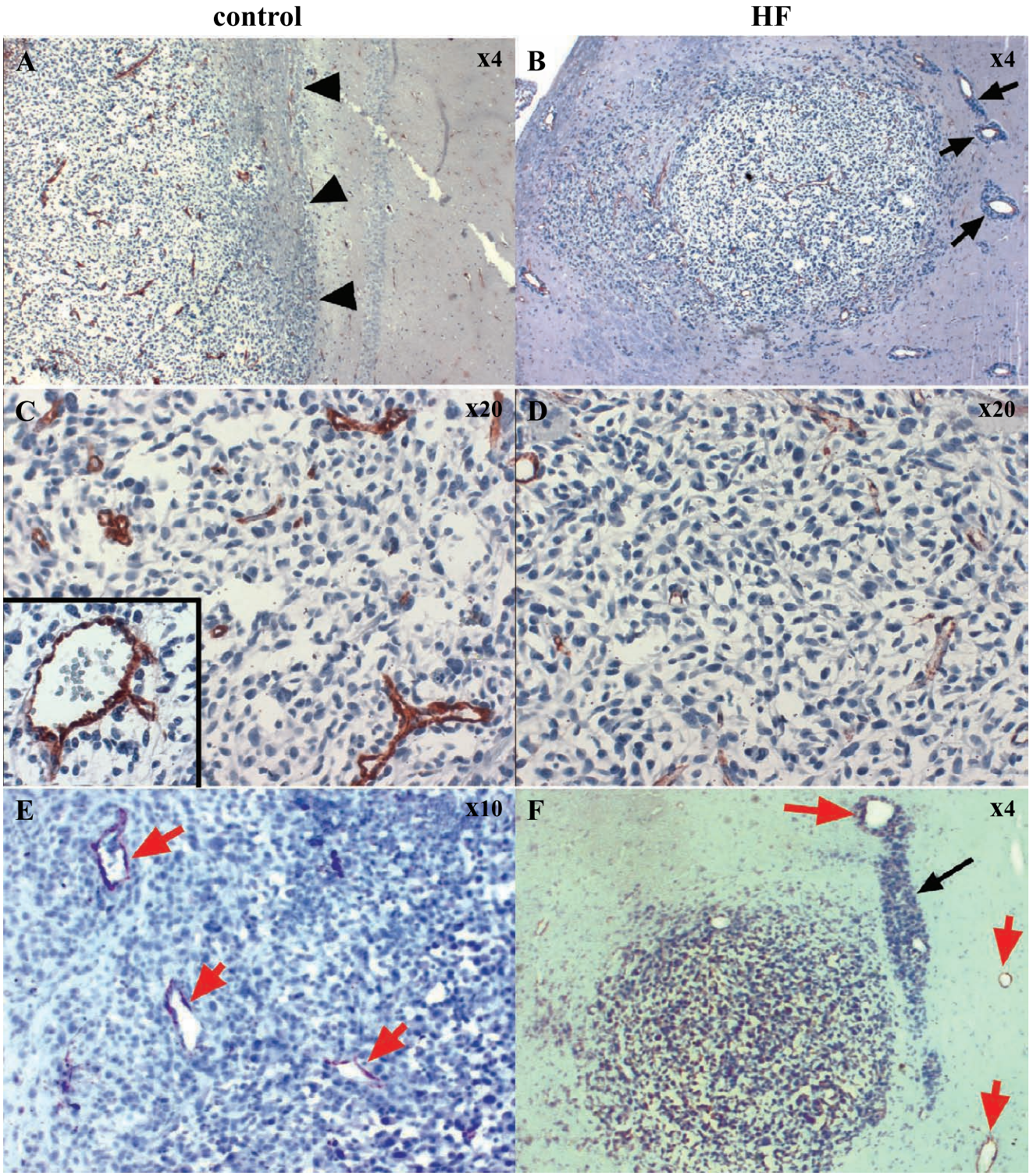


**Figure 4.** *Effect of HF on vessel density and maturation in metastatic brain tumors. Fischer rats were inoculated with malignant fibrous histiocytoma. Oral treatment with HF (0.4 mg/kg per day) or control vehicle was initiated on day 6 after tumor implantation, and treatment was repeated daily. On days 14 and 19, tumor samples were collected for histologic examination. Representative slides of control tumors (A, C, E) and HF-treated tumors (B, D, F) obtained on day 14 are presented. (A–D) Anti–factor VIII (vWF) immunostaining of control (A and C) and HF-treated (B and D) rats. Black arrows indicate vessel cooption phenomena, and arrowheads mark the well-defined borders of control tumor. (E and F) Anti-SMA immunostaining of control (E) and HF-treated (F) rats. Red arrows mark blood vessels stained positively with α-SMA antibody. Magnification is indicated on top of each figure.*

demonstrate that HF, an antiangiogenic compound, increased satellite tumors and vessel cooption in our metastatic brain tumor model. There are two previous publications [46,47] that have shown that anti-VEGF treatment increased invasiveness and cooption of host vessels in models of glioblastoma. This suggests that in the therapeutic situation, where angiogenesis is inhibited, a blockade of neovascularization favors vessel cooption. Moreover, this seems to be

independent of the antiangiogenic mechanism of action (anti-VEGF *versus* HF inhibitory affect on collagen I synthesis). In addition, this indulgence of invasiveness seems to occur across all tumor types even in a metastatic tumor that usually tends to grow as a well-defined mass. We should emphasize that with anti-VEGF antibody, there was a 23-fold increase in satellite tumor mass [46], and with DC101, an antibody against VEGF receptor-2, there was a fivefold increase in the number of satellites [47], whereas with HF, we observed only a 2.4-fold increase. Thus, the antitumor effect of HF, in addition to its antiangiogenic effect, seems to moderate the cooption effect.

In summary, we have shown that systemic treatment with HF inhibits the growth and vascularization of metastatic brain tumors and concurrently prolonged the survival of the animals, yet moderately increased tumor cooption and invasiveness along host vessels. Apparently, it seems that for better anticancer effect, there is a need to combine additional therapeutic modalities such as concomitant use of chemotherapy or other newly evolving biologic therapies. However, in the CNS, such combinations are particularly challenging due to the limitations posed by the blood–brain barrier. The possibility of combining HF with radiation therapy needs further investigation because radiosensitivity depends on oxygenation. Further studies are needed to evaluate appropriate combinations, dosing, and schedule of such therapeutic approaches in both primary and metastatic brain tumors.

### Acknowledgements

We thank Eithan Galun (Hadassah University Hospital) for helpful discussions.

## References

[1] Bernsen HJJA and Van der Kogel AJ (1999). Antiangiogenic therapy in brain tumor models. *J Neuro-Oncol* **45,** 247–255.

[2] Reijneveld JC, Voest EE, and Taphoorn MJB (2000). Angiogenesis in malignant primary and metastatic brain tumors. *J Neurol* **247,** 597–608.

[3] Folkman J (1985). Tumor angiogenesis. *Adv Cancer Res* **43,**175–203.

[4] Vidal S, Kovacs K, Lloyd RV, Meyer FB, and Scheithauer BW (2002). Angiogenesis in patients with craniopharyngiomas correlation with treatment and outcome. *Cancer* **94,** 738–745.

[5] Vidal S, Kovacs K, Horvath E, Scheithauer BW, Turoki T, and Lloyd RV (2001). Microvessel density in pituitary adenomas and carcinomas. *Virchows Arch* **438,** 595–602.

[6] Korkolopoulou P, Patsouris E, Kavantzas N, Konstantinidou AE, Christodoulou P, Thomas-Tsagli E, Pananikolaou A, Eftychiadis C, Pavlopoulos PM, Angelidakis D, Rologis D, and Davaris P (2002). Prognostic implications of microvessel morphometry in diffuse astrocytic neoplasms. *Neuropathol Appl Neurobiol* **28,** 57–66.

[7] Iruela-Arispe ML, Hasselaar P, and Sage H (1991). Differential expression of extracellular matrix proteins is correlated with angiogenesis in vitro. *Lab Invest* **64,** 174–186.

[8] Iruela-Arispe ML, Diglio CA, and Sage H (1991). Modulation of extracellular matrix proteins by endothelial cells undergoing angiogenesis *in vitro*. *Arterioscler Thromb* **11,** 805–815.

[9] Madri JA and Sten KS (1982). Aortic endothelial cell migration I matrix requirements and composition. *Am J Pathol* **106,** 180–186.

[10] Montesano R, Orci L, and Vassalli P (1983). *In vitro* rapid organization of endothelial cells into capillary-like networks is promoted by collagen matrices. *J Cell Biol* **97,** 1648–1652.

[11] Jackson CJ and Jenkins KL (1991). Type I collagen fibrils promote rapid vascular tube formation upon contact with the apical side of cultured endothelium. *Exp Cell Res* **192,** 319–323.

[12] Senger DR, Claffey KP, Benes JE, Perruzzi CA, and Sergiou A (1997). Angiogenesis promoted by vascular endothelial growth factor: regulation through a1b1 and a2b1 integrins. *Proc Natl Acad Sci USA* **94,** 13612–13617.

[13] Pines M, Vlodavsky I, and Nagler A (2000). Halofuginone: from veterinary use to human therapy. *Drug Dev Res* **50,** 371–378.

[14] Pines M and Nagler A (1997). Halofuginone—a novel anti-fibrotic therapy. *Gen Pharmacol* **30,** 445–450.

[15] Elkin M, Miao HQ, Nagler A, Aingorn E, Reich R, Hemo I, Dou HL, Pines M, and Vlodavsky I (2000). Halofuginone: a potent inhibitor of critical steps in angiogenesis progression. *FASEB J* **14,** 2477–2485.

[16] Abramovitch R, Dafni H, Neeman M, and Nagler A (1999). Inhibition of neovascularization and tumor growth, and facilitation of wound repair, by halofuginone, an inhibitor of collagen type I synthesis. *Neoplasia* **1,** 321–329.

[17] Gavish Z, Pinthus JH, Barak V, Ramon J, Nagler A, Eshhar Z, and Pines M (2002). Growth inhibition of prostate cancer xenografts by halofuginone. *Prostate* **51,** 73–83.

[18] Boehm T, Folkman J, Browder T, and O'Reilly MS (1997). Antiangiogenic therapy of experimental cancer does not induce acquired drug resistance. *Nature* **390,** 404–407.

[19] Millauer B, Shwver LK, Plate KH, Risau W, and Ullrich A (1994). Glioblastoma growth inhibited *in vivo* by a dominant-negative *Flk-1* mutant. *Nature* **367,** 576–579.

[20] O'Reilly MS, Holmgren L, Chen C, and Folkman J (1996). Angiogstatin induces and sustains dormancy of human primary tumors in mice. *Nat Med* **2,** 689–692.

[21] Holash J, Maisonpierre PC, Compon D, Boland P, Alexander CR, Zagzag D, and Yancopoulos GD (1999). Vessel cooption, regression, and growth in tumors mediated by angiopoietins and VEGF. *Science* **284,** 1994–1998.

[22] Kusters B, Leenders WPJ, Wesseling P, Smits D, Verrijp K, Ruiter DJ, Peters JPW, Van der Kogel AJ, and de Waal RMW (2002). Vascular endothelial growth factor-A165 induces progression of melanoma brain metastases without induction of sprouting angiogenesis. *Cancer Res* **62,** 341–345.

[23] Siegal T, Horowitz A, and Gabizone A (1995). Doxorubicin encapsulated in sterically stabilized liposomes for the treatment of a brain tumor model: biodistribution and therapeutic efficacy. *J Neurosurg* **83,** 1029–1037.

[24] Shoshan Y and Siegal T (1996). Control of vasogenic edema in a brain tumor model: comparison between dexamethasone and superoxide dismutase. *Neurosurgery* **39,** 1206–1213.

[25] Zhou R, Mazurchuk R, and Straubinger RM (2002). Antivasculature effects of doxorubicin-containing liposomes in an intracranial rat brain tumor model. *Cancer Res* **62,** 2561–2566.

[26] Ross BD, Chenevert TL, Garwood M, Kim B, Stegman LD, Ben-Yoseph O, Zwolshen J, Rehemtulla A, and Sunkara PS (2003). Evaluation of (E)-2′-deoxy-2′-(fluoromethylene)cytidine on the 9L rat brain tumor model using MRI. *NMR Biomed* **16,** 67–76.

[27] Kish PE, Blaivas M, Strawderman M, Muraszko KM, Ross DA, Ross BD, and McMahon G (2001). Magnetic resonance imaging of ethylnitrosourea–induced rat gliomas: a model for experimental therapeutics of low-grade gliomas. *J Neuro-Oncol* **53,** 243–257.

[28] Gossmann A, Helbich TH, Kuriyama N, Ostrowitzki S, Roberts TP, Shames DM, van Bruggen N, Wendland MF, Israel MA, and Brasch RC (2002). Dynamic contrast-enhanced magnetic resonance imaging as a surrogate marker of tumor response to anti-angiogenic therapy in a xenograft model of glioblastoma multiforme. *J Magn Reson Imaging* **15,** 233–240.

[29] Leenders W, Kusters B, Pikkemaat J, Wesseling P, Ruiter D, Heerschap A, Barentsz J, and de Waal RM (2003). Vascular endothelial growth factor-A determines detectability of experimental melanoma brain metastasis in GD-DTPA–enhanced MRI. *Int J Cancer* **105,** 437–443.

[30] Cha S, Johnson G, Wadghiri YZ, Jin O, Babb J, Zagzag D, and Turnbull DH (2003). Dynamic, contrast-enhanced perfusion MRI in mouse gliomas: correlation with histopathology. *Magn Reson Med* **49,** 848–855.

[31] Robinson SP, McIntyre DJ, Checkley D, Tessier JJ, Howe FA, Griffiths JR, Ashton SE, Ryan AJ, Blakey DC, and Waterton JC (2003). Tumour dose response to the antivascular agent ZD6126 assessed by magnetic resonance imaging. *Br J Cancer* **88,** 1592–1597.

[32] Chenevert TL, Meyer CR, Moffat BA, Rehemtulla A, Mukherji SK, Gebarski SS, Quint DJ, Robertson PL, Lawrence TS, Junck L, Taylor JM, Johnson TD, Dong Q, Muraszko KM, Brunberg JA, and Ross BD (2002). Diffusion MRI: a new strategy for assessment of cancer therapeutic efficacy. *Mol Imaging* **1,** 336–343.

[33] Tailor DR, Roy A, Regatte RR, Charagundla SR, McLaughlin AC, Leigh JS, and Reddy R (2003). Indirect 17(*O*)-magnetic resonance imaging of cerebral blood flow in the rat. *Magn Reson Med* **49,** 479–487.

[34] Robinson SP, Rijken PF, Howe FA, McSheehy PM, van der Sanden BP, Heerschap A, Stubbs M, Van der Kogel AJ, and Griffiths JR (2003). Tumor vascular architecture and function evaluated by non-invasive susceptibility MRI methods and immunohistochemistry. *J Magn Reson Imaging* **17,** 445–454.

[35] Abramovitch R, Dafni H, Smouha E, Benjamin LE, and Neeman M (1999). *In vivo* prediction of vascular susceptibility to vascular endothelial growth factor withdrawal: magnetic resonance imaging of C6 rat glioma in nude mice. *Cancer Res* **59,** 5012–5016.

[36] Ogawa S, Lee TM, Kay AR, and Tank DW (1990). Brain magnetic resonance imaging with contrast dependent on blood oxygenation. *Proc Natl Acad Sci USA* **87,** 9868–9872.

[37] van Zijl PC, Eleff SM, Ulatowski JA, Oja JM, Ulug AM, Traystman RJ, and Kauppinen RA (1998). Quantitative assessment of blood flow, blood volume and blood oxygenation effects in functional magnetic resonance imaging. *Nat Med* **4,** 159–167.

[38] Goldshmidt O, Zcharia E, Abramovitch R, Metzger S, Guatta-Rangini Z, Aingorn H, Friedmann Y, Mitrani E, and Vlodavsky I (2002). Cell surface expression and secretion of heparanase markedly promote tumor angiogenesis and metastasis. *Proc Natl Acad Sci USA* **99,** 10031–10036.

[39] Ross BD, Zhao YJ, Neal ER, Stegman LD, Ercolani M, Ben-Yoseph O, and Chenevert TL (1998). Contributions of cell kill and posttreatment tumor growth rates to the repopulation of intracerebral 9L tumors after chemotherapy: an MRI study. *Proc Natl Acad Sci USA* **95,** 7012–7017.

[40] Abramovitch R, Frenkiel D, and Neeman M (1998). Analysis of subcutaneous angiogenesis by gradient echo magnetic resonance imaging. *Magn Reson Med* **39,** 813–824.

[41] Siegal T, Rubinstein R, Tzuk-Shina T, and Gomori JM (1997). Utility of relative cerebral blood volume mapping derived from perfusion magnetic resonance imaging in the routine follow up of brain tumors. *J Neurosurg* **86,** 22–27.

[42] Benjamin LE, Golijanin D, Itin A, Pode D, and Keshet E (1999). Selective ablation of immature blood vessels in established human tumors follows vascular endothelial growth factor withdrawal. *J Clin Invest* **103,** 159–165.

[43] Gross DJ, Reibstein I, Weiss L, Slavin S, Stein I, Neeman M, Abramovitch R, and Benjamin LE (1999). The antiangiogenic agent linomide inhibits the growth rate of von Hippel-Lindau paraganglioma xenografts to mice. *Clin Cancer Res* **5,** 3669–3675.

[44] Blouw B, Song H, Tihan T, Bosze J, Ferrara N, Gerber HP, Johnson RS, and Bergers G (2003). The hypoxic response of tumors is dependent on their microenvironment. *Cancer Cell* **4,** 133–146.

[45] Bergers G and Benjamin LE (2003). Tumorigenesis and the angiogenic switch. *Nat Rev Cancer* **3,** 401–410.

[46] Rubenstein JL, Kim J, Ozawa T, Zhang M, Westphal M, Deen DF, and Shuman MA (2000). Anti-VEGF antibody treatment of glioblastoma prolongs survival but results in increased vascular cooption. *Neoplasia* **2,** 306–314.

[47] Kunkel P, Ulbricht U, Bohlen P, Brockmann MA, Fillbrandt R, Stavrou D, Westphal M, and Lamszus K (2001). Inhibition of glioma angiogenesis and growth *in vivo* by systemic treatment with a monoclonal antibody against vascular endothelial growth factor receptor-2. *Cancer Res* **61,** 6624–6628.